Received: 9 August 2017 | Revised: 30 December 2017 | Accepted: 13 March 2018

DOI: 10.1002/term.2664

RESEARCH ARTICLE

WILEY

Bone morphogenetic protein-2 release profile modulates bone formation in phosphorylated hydrogel

Maurits G.L. Olthof[1,2,4,5] | Diederik H.R. Kempen[3] | Xifeng Liu[1,2] | Mahrokh Dadsetan[1,2] | Marianna A. Tryfonidou[4] | Michael J. Yaszemski[1,2] | Wouter J.A. Dhert[4,5] | Lichun Lu[1,2]

[1] Department of Physiology and Biomedical Engineering, Mayo Clinic College of Medicine, Rochester, MN, USA

[2] Department of Orthopedic Surgery, Mayo Clinic College of Medicine, Rochester, MN, USA

[3] Department of Orthopaedic Surgery, Onze Lieve Vrouwe Gasthuis, Amsterdam, The Netherlands

[4] Faculty of Veterinary Medicine, Utrecht University, Utrecht, The Netherlands

[5] Department of Orthopaedics, University Medical Center, Utrecht, The Netherlands

Correspondence
Lichun Lu, Department of Physiology and Biomedical Engineering, Mayo Clinic College of Medicine, 200 First Street SW, MS 3-69, Rochester, MN 55905, USA.
Email: lu.lichun@mayo.edu

Funding information
AO Foundation, Grant/Award Number: AO startup grant S-15-46K; National Institutes of Health, Grant/Award Numbers: R01 EB03060 and R01 AR45871; Anna-NOREF Foundation; Dutch Arthritis Foundation, Grant/Award Number: LLP22

Abstract

The optimal release profile of locally delivered bone morphogenetic protein-2 (BMP-2) for safe and effective clinical application is unknown. In this work, the effect of differential BMP-2 release on bone formation was investigated using a novel biomaterial oligo[(polyethylene glycol) fumarate] bis[2-(methacryloyloxy) ethyl] phosphate hydrogel (OPF-BP) containing poly(lactic-*co*-glycolic acid) microspheres. Three composite implants with the same biomaterial chemistry and structure but different BMP-loading methods were created: BMP-2 encapsulated in microspheres (OPF-BP-Msp), BMP-2 encapsulated in microspheres and adsorbed on the phosphorylated hydrogel (OPF-BP-Cmb), and BMP-2 adsorbed on the phosphorylated hydrogel (OPF-BP-Ads). These composites were compared with the clinically used BMP-2 carrier, Infuse® absorbable collagen sponge (ACS). Differential release profiles of bioactive BMP-2 were achieved by these composites. In a rat subcutaneous implantation model, OPF-BP-Ads and ACS generated a large BMP-2 burst release (>75%), whereas a more sustained release was seen for OPF-BP-Msp and OPF-BP-Cmb (~25% and 50% burst, respectively). OPF-BP-Ads generated significantly more bone than did all other composites, and the bone formation was 12-fold higher than that of the clinically used ACS. Overall, this study clearly shows that BMP-2 burst release generates more subcutaneous bone than do sustained release in OPF-BP-microsphere composites. Furthermore, composites should not only function as a delivery vehicle but also provide a proper framework to achieve appropriate bone formation.

KEYWORDS

biomaterials, bone morphogenetic protein-2 release, bone tissue engineering, oligo[(polyethylene glycol) fumarate], poly(lactic-*co*-glycolic acid)

1 | INTRODUCTION

Bone morphogenetic protein-2 (BMP-2), a well-known stimulus for bone formation, has already been extensively used in clinical applications. Despite more than a decade of clinical experience, the results of many clinical trials have been rather disappointing considering the impressive preclinical results in numerous species and application sites (Seeherman, Li, & Wozney, 2003). In humans, the effectiveness of BMP-2 has been demonstrated in limited clinical cases. For example, addition of BMP-2 was as effective as autografts for open tibial fracture with reamed intramedullary nail fixation and fracture nonunions (Aro et al., 2011; Garrison et al., 2007). For spine fusion, the use of BMP-2 was shown to be more effective than autogenous bone graft in terms of radiographic spinal fusion and clinical improvement only in patients undergoing fusion for single-level degenerative disk disease (Garrison et al., 2007)

Apart from the limited effectiveness in clinical applications, many serious complications have emerged related to the use of BMP-2

(Benglis, Wang, & Levi, 2008; Carragee, Hurwitz, & Weiner, 2011). As these complications were observed less frequently when lower BMP-2 amounts were implanted, they can be partially attributed to the supraphysiological BMP-2 dosage used in current clinical applications (Dickerman et al., 2007; Tumialan, Pan, Rodts, & Mummaneni, 2008). Therefore, current research strategies have focused on optimizing biomaterials for local delivery to enhance the site-specific osteogenic and osteoinductive effects of BMP-2.

Despite the extensive research on BMP-2 carrier development for bone regeneration, the optimal growth factor dose, release duration, and required timing of release are still unknown. Although optimizing these release parameters is a logical step in improving BMP-2 therapies, this process is difficult because adjustments of the growth factor release rate often require changes to the composite structure or composition and hence may influence cellular behaviour and subsequent bone formation. This phenomenon has indeed been noticed in previous studies (Takita et al., 2004; Tazaki et al., 2009; Uludag, D'augusta, Palmer, Timony, & Wozney, 1999; Yamamoto, Ikada, & Tabata, 2001; Yamamoto, Takahashi, & Tabata, 2003). Optimizing BMP-2 release kinetics could increase the growth factor's efficacy, lower the required dose, and minimize complications in the clinics. Therefore, the main aim of this study was to investigate the effect of different BMP-2 release profiles on bone formation in a biomaterial with tailorable BMP-2 release kinetics without altering biomaterial chemistry and structure. As discussed earlier, apart from BMP-2 release kinetics, also the biomaterial physical and chemical properties can stimulate the BMP-2-induced bone formation. Therefore, the second aim of this study was to compare the newly developed phosphorylated hydrogel with the golden standard delivery vehicle for BMP-2, the Infuse® absorbable collagen sponge (ACS).

A novel oligo[(polyethylene glycol) fumarate] bis[2-(methacryloyloxy) ethyl] phosphate hydrogel (OPF-BP) containing poly(lactic-*co*-glycolic acid) (PLGA) microspheres was developed to investigate the effect of BMP-2 release on bone formation. In vitro phosphorylated OPF-BP showed improved attachment, proliferation, and differentiation of osteogenic precursor cells and mesenchymal stem cells than does nonphosphorylated OPF (Dadsetan et al., 2012). To tailor the release, BMP-2 was adsorbed in the composite matrix and/or encapsulated in the microspheres. We hypothesized that adsorption will result in a large burst release with subsequent low-dose sustained release whereas microsphere encapsulation will result in a more sustained release of BMP-2 over time. By altering the BMP-2 adsorption/microsphere encapsulation ratio without adjusting the biomaterial chemistry and structure, changes in bone formation can be ascribed to the differential BMP-2 release. Furthermore, OPF-BP was compared with ACS with similar BMP-2 release kinetics to analyze the effect of the biomaterial properties.

2 | MATERIALS AND METHODS

2.1 | Experimental design

OPF-BP composites with a 75% porosity containing 2.5% (w/w) PLGA microspheres were employed. To assess the effect of differential BMP-2 release profiles on bone formation, BMP-2 (Medtronic, Minneapolis, MN) was either adsorbed on the OPF-BP hydrogel to achieve a burst release or encapsulated in PLGA microspheres to achieve a more sustained release profile. A schematic design of the fabrication process is shown in Figure 1a. Three different composite implants were created: 100% of the BMP-2 encapsulated in PLGA microspheres (OPF-BP-Msp: microspheres; Figure 1b), 50% of the BMP-2 encapsulated in PLGA microspheres and 50% adsorbed on the composite (OPF-BP-Cmb: combined; Figure 1c), and 100% adsorbed on the composite (OPF-BP-Ads: adsorbed; Figure 1d). To compare these composite designs with the clinically used BMP-2 carrier, Infuse® ACS (Medtronic, Minneapolis, MN) was used.

The effect of the different protein incorporation methods on BMP-2 release was assessed in vitro and in vivo by employing BMP-2 radiolabelled with ^{125}I. The in vivo bioactivity was investigated by analyzing bone formation after 9 weeks of subcutaneous implantation in rats.

2.2 | BMP-2 radioiodination

Carrier-free Na^{125}I was obtained from PerkinElmer Life and Analytical Sciences (Boston, MA). To study the release profiles of BMP-2, a fraction of the incorporated BMP-2 was radiolabelled with ^{125}I, using the chloramine-T method as previously described (Poduslo, Curran, & Berg, 1994). The radiolabelled BMP-2 was separated from the free ^{125}I by 24-hr dialysis with a 10-kDa molecular weight cut-off (SpectraPor 7, Rancho Dominguez, CA), against 0.01 M phosphate-buffered saline at pH 7.4 (Sigma-Aldrich, St. Louis, MO). The ^{125}I-BMP-2 dialysate was concentrated in a Millipore device (10-kDa molecular weight cut-off, Billerica, MA), and the purity was determined by trichloroacetic acid precipitation. The final ^{125}I-BMP-2 preparation contained 99.7% precipitable counts, which indicated the percentage of covalently bound ^{125}I to the BMP-2. Thereafter, ^{125}I-BMP-2 was mixed with nonlabelled BMP-2 (1:5.3 hot/cold ratio) and incorporated into the composite formulations.

2.3 | Microsphere fabrication

PLGA microspheres (50:50 lactic to glycolic acid ratio, M_w = 52 kDa; Lakeshore Biomaterials, AL) were fabricated using a water-in-oil-in-water double-emulsion solvent-extraction technique according to a previously described method (Kempen et al., 2008a). Briefly, an aqueous solution containing 130 (OPF-BP-Msp), 65 (OPF-BP-Cmb), or 0 μl (OPF-BP-Ads) of 3.7 mg/ml ^{125}I-BMP-2/BMP-2 (1:5.3 hot/cold ratio) solution was emulsified with 250 mg PLGA 50:50 dissolved in 1.25 ml of dichloromethane using a vortex at 3,050 rpm. The solution was re-emulsified in 2 ml of 2% (w/v) aqueous poly(vinyl alcohol) (87–89% mole hydrolyzed, M_w = 13,000–23,000, Sigma-Aldrich) to create the double emulsion and added to 100 ml of a 0.3% (w/v) poly(-vinyl alcohol) solution and 100 ml of a 2% (w/v) aqueous isopropanol solution. After 1 hr of slow stirring, the PLGA microspheres were collected by centrifugation at 2,500 rpm for 3 min, washed three times with distilled deionized water (ddH_2O), and freeze dried to a free-flowing powder. After freeze drying, the morphology of the

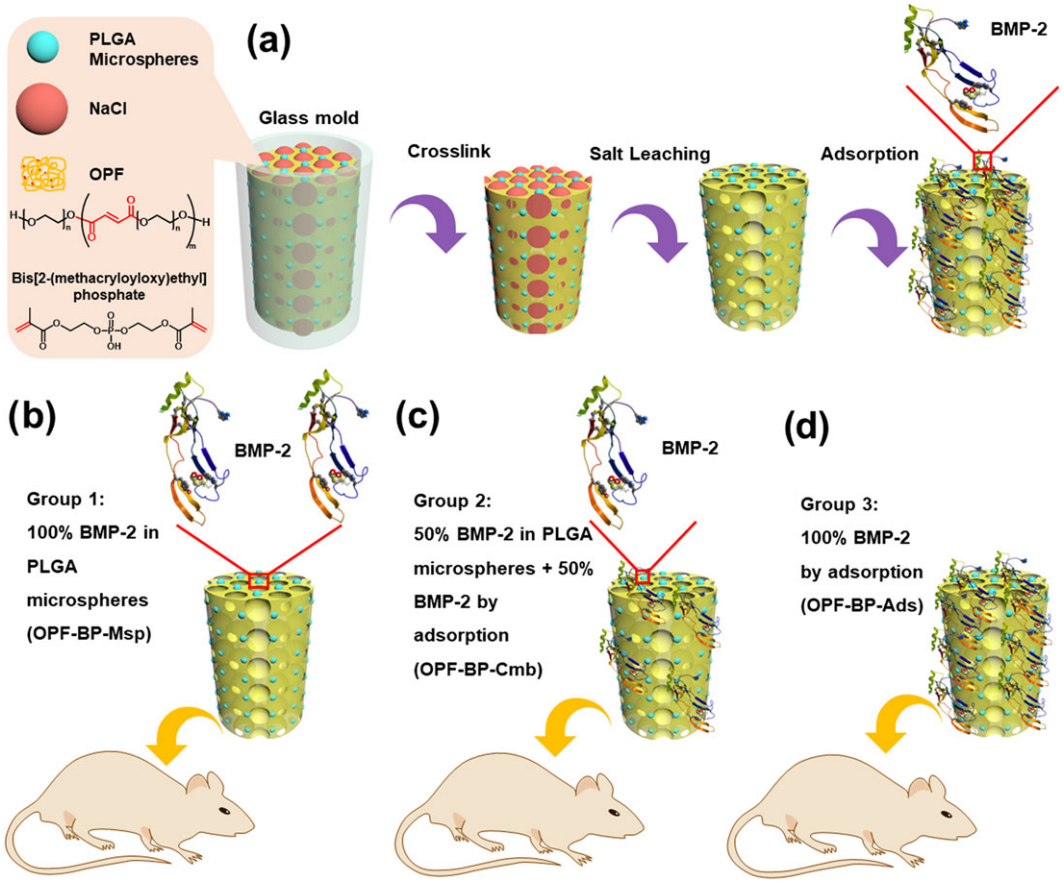

FIGURE 1 (a) Scheme for fabrication procedures of the OPF-BP composite implants. Three types of implants with BMP-2 incorporated by varied loading methods were created: (b) BMP-2 encapsulated in microspheres (OPF-BP-Msp), (c) BMP-2 encapsulated in microspheres and adsorbed on the hydrogel (OPF-BP-Cmb), and (d) BMP-2 adsorbed on the hydrogel (OPF-BP-Ads). BMP-2, bone morphogenetic protein-2; OPF, oligo[(polyethylene glycol) fumarate]; PLGA, poly(lactic-*co*-glycolic acid) [Colour figure can be viewed at wileyonlinelibrary.com]

microspheres was observed by scanning electron microscopy (SEM; S-4700, Hitachi Instruments, Tokyo, Japan) at 5.0 kV.

2.4 | Fabrication of composites

OPF was fabricated using polyethylene glycol with an initial molecular weight of 10 kDa according to a previously described method (Dadsetan et al., 2012). BP (Aldrich, Milwaukee, WI) was cross-linked into the OPF hydrogel. To create the hydrogel composites, OPF (41% w/w), *N*-vinyl pyrrolidinone (NVP; 29% w/w, Sigma-Aldrich, St. Louis, MO), BP (8.2% w/w), and Irgacure 2959 (0.2% w/w, Ciba Specialty Chemicals, Tarrytown, NY) were dissolved in ddH_2O (21.6% w/w). The resulting OPF/NVP/BP paste (22.5% w/w) was mixed with NaCl salt particles (75% w/w, sieved to a maximum size of 300 μm) and PLGA microspheres (2.5% w/w). The mixture was then forced into a cylindrical glass mould with a diameter of 3.5 mm and exposed to UV light (365 nm at intensity of ~8 mW/cm^2; Blak-Ray model 100AP, Upland, CA) to cross-link the composites for 40 min. The composites were cut into 6-mm-long rods and immerged in sterile ddH_2O to leach out the salt. After blot drying, the additional BMP-2 was adsorbed on the composite matrix. The Infuse® ACS was cut into cylindrical (4 mm in diameter and 6 mm in length) rods using a tissue puncher and loaded with ^{125}I-BMP-2 using adsorption. To analyze the morphological features of the OPF hydrogels, dry (directly after cross-linking) and hydrated samples were freeze dried and observed by SEM at 5 kV.

2.5 | In vitro BMP-2 release

The in vitro release of BMP-2 was analyzed as previously described (Kempen et al., 2008b). Briefly, composite implants placed in a 12-well transwell culture system were exposed to consecutive 7-day W20-17 cell cultures in Dulbecco's modified Eagle's medium/Nutrient Mixture F-12 Ham 1:1 mixture (Sigma-Aldrich, St. Louis, MO) containing 10% foetal bovine serum and 1% penicillin. The medium was analyzed weekly for radiolabelled ^{125}I-BMP using a gamma counter. After 9 weeks, the composites were collected to determine the remaining activity. The ^{125}I activity was corrected for decay and normalized to the starting amount. The counts per minute were correlated to the amount of released BMP-2.

2.6 | In vitro biological activity

OPF-BP-Msp, OPF-BP-Ads, and OPF-BP control (unloaded OPF-BP implant) were tested using ATDC5 cells, a well-known culture system that undergoes late-phase osteogenic differentiation and is often employed for determination of BMP activity (Matsumoto et al., 2012; Shukunami, Ohta, Sakuda, & Hiraki, 1998; Yao & Wang,

2013). They encompass stages from mesenchymal condensation to calcification and as such representative of endochondral bone formation. In fracture healing (and specifically large bone defects), this is the primary process of bone regeneration. In order to determine whether biologically active BMP-2 was released even after 9 week of implantation, the implants were placed in Dulbecco's modified Eagle's medium containing 10% foetal bovine serum, 1% penicillin/streptomycin, and 1% human serum albumin during this period. Thereafter, the implants were exposed to 200 µl of fresh media for 2 weeks. The conditioned medium was collected at 11 weeks and stored at −80 °C until further analysis. Subconfluent ATDC5 cells were exposed to the conditioned medium for 3 days, after which the cells were lysed and assessed for alkaline phosphatase (ALP) activity and total DNA content using ALP assay kit (Sigma) and Qubit (Life Technologies) according to the manufacturer's instructions, respectively. The ALP activity was normalized over total DNA content and compared with the negative control (i.e., ATDC5 cells cultured in conditioned media with unloaded OPF-BP control). Freshly added BMP-2 to ATDC5 cells with a range of expected BMP-2 release concentrations (0, 0.025, 0.05, 0.1, and 1 µg BMP-2/ml) served as a positive control.

2.7 | Animals and surgical procedure

Twenty-two 12-week-old male Harlan Sprague Dawley rats were used for this study according to an approved protocol by the local animal care and use committee. Surgery was performed under sterile conditions and general anaesthesia (45/10 mg/kg ketamine/xylazine). After shaving and disinfecting the surgical sites, we created subcutaneous pockets in each limb and filled them with ^{125}I-BMP-2 labelled implants. Two subcutaneous pockets in the thoracolumbar region were used to implant the controls (unloaded implants). Acetaminophen (160 mg in 5 ml added to one pint water bottle) was given as post-operative analgesia for the duration of 1 week. Fluorochrome markers calcein green (10 mg/kg, intraperitoneal) and tetracycline (10 mg/kg, intraperitoneal) were administered at 3 and 6 weeks post-operatively, respectively. After 9 weeks, the rats were euthanized by CO_2 asphyxiation to collect the implants for assessment of bone formation by micro-computed tomography (µCT) and subsequent histological analysis.

2.8 | In vivo BMP-2 release

Four scintillation probes (model 44-3 low-energy gamma scintillator; Ludlum Measurements Inc., TX) connected to digital scalers as described previously (Kempen et al., 2008a) were used for noninvasive determination of in vivo ^{125}I-BMP-2 release kinetics. Directly after wound closure, the ^{125}I-BMP-2 activity was measured to obtain the starting implanted dose. At each subsequent time-point, the rats were anesthetized using isoflurane (1.5–4%) to measure the local ^{125}I-BMP-2 activity over two 1-min periods with two different detectors. To determine the BMP-2 release, the ^{125}I-BMP-2 measurements were corrected for radioactive decay and background activity. The ^{125}I-BMP-2 activity was normalized to the starting implanted dose to determine the retained ^{125}I-BMP-2 dose and released amounts.

2.9 | In vivo bioactivity of released BMP-2

Micro-computed tomography was used to measure the total bone volume in the composites. Ex vivo scanning of the composites was performed using a Scanco µCT 35 scanner (Scanco Medical, Switzerland) at 10-µm resolution. The samples were loaded in a cylinder, and standardized settings were used for all scans. Standardized thresholds were used to quantify the ectopic calcified tissue.

2.10 | Histology

The samples were dehydrated in graded series of ethanol and embedded in methyl methacrylate for qualitative assessment by histology. Sections were stained with Gömöri trichrome for evaluation of the general tissue response and bone formation. The stained sections were analyzed by a board-eligible veterinary pathologist. Unstained sections were used for fluorescence microscopy to evaluate fluorochrome incorporation.

2.11 | Statistical analysis

Statistical analysis was performed using SPSS 22.0 software (SPPS Inc., Chicago, IL). In vitro results (n = 3) and in vivo results (n = 8) are given as means ± standard deviations (*SD*s). Prior to the in vivo study, power analysis estimated that in order to demonstrate a relevant difference of at least 20% at an α of .05 and an *SD* of 1.4, the groups should be n = 8 per condition at a power of 80%. Extra available subcutaneous locations were filled with OPF-BP-Cmb and ACS (n = 10). All datasets were tested for outliers using studentized residuals, for normality of the residuals using the Shapiro–Wilk test and for homogeneity of variances using the Levene test. Nonparametric data were analyzed with Kruskal–Wallis and Benjamini–Hochberg post hoc tests. Parametric data were analyzed with univariate analyses of variance followed by Benjamini–Hochberg post hoc (homogeneous variances) or Games–Howell post hoc (unequal variances). Differences were considered significant for $p < .05$. With in vitro bioactivity assays, >25 ng BMP-2 per ml was considered a relevant difference. For in vivo BMP-2 release, differences were considered relevant at >100 ng BMP-2 (Gruber, Weich, Dullin, & Schliephake, 2009; Tazaki et al., 2009).

3 | RESULTS

3.1 | BMP-2 labelling and scaffold characterization

Labelling of the BMP-2 with ^{125}I resulted in an activity per mass of 6.1 µCi/µg. The microspheres were loaded with 2.9 and 1.3 µg BMP-2/mg PLGA for the OPF-BP-Msp and OPF-BP-Cmb groups, respectively. The characteristics of three composites are summarized in Table 1. The different loading methods resulted in no significant differences of total BMP-2 loading per composite.

A schematic demonstration of the loading procedure of BMP-2 into PLGA microspheres is presented in Figure 2a. SEM of PLGA microspheres with or without the incorporation of BMP-2 proteins was conducted after freeze drying of the microspheres. As demonstrated in Figure 2, the unloaded (Figure 2a) and BMP-2-loaded (Figure 2b) PLGA microspheres showed a smooth surface. The

TABLE 1 Implant characteristics

Composite name	BMP loading		Initial activity/implant (μCi)	BMP-2/implant (μg)
	Hydrogel	Microspheres		
OPF-BP-Msp	0% absorbed on hydrogel	100% loaded in microspheres	3.1 ± 0.1	4.0 ± 0.1
OPF-BP-Cmb	50% absorbed on hydrogel	50% loaded in microspheres	3.0 ± 0.2	3.9 ± 0.3
OPF-BP-Ads	100% loaded on hydrogel	Empty microspheres	3.1 ± 0.6	4.0 ± 0.7

Note. BMP = bone morphogenetic protein; OPF-BP = oligo[(polyethylene glycol) fumarate] bis[2-(methacryloyloxy) ethyl] phosphate hydrogel.

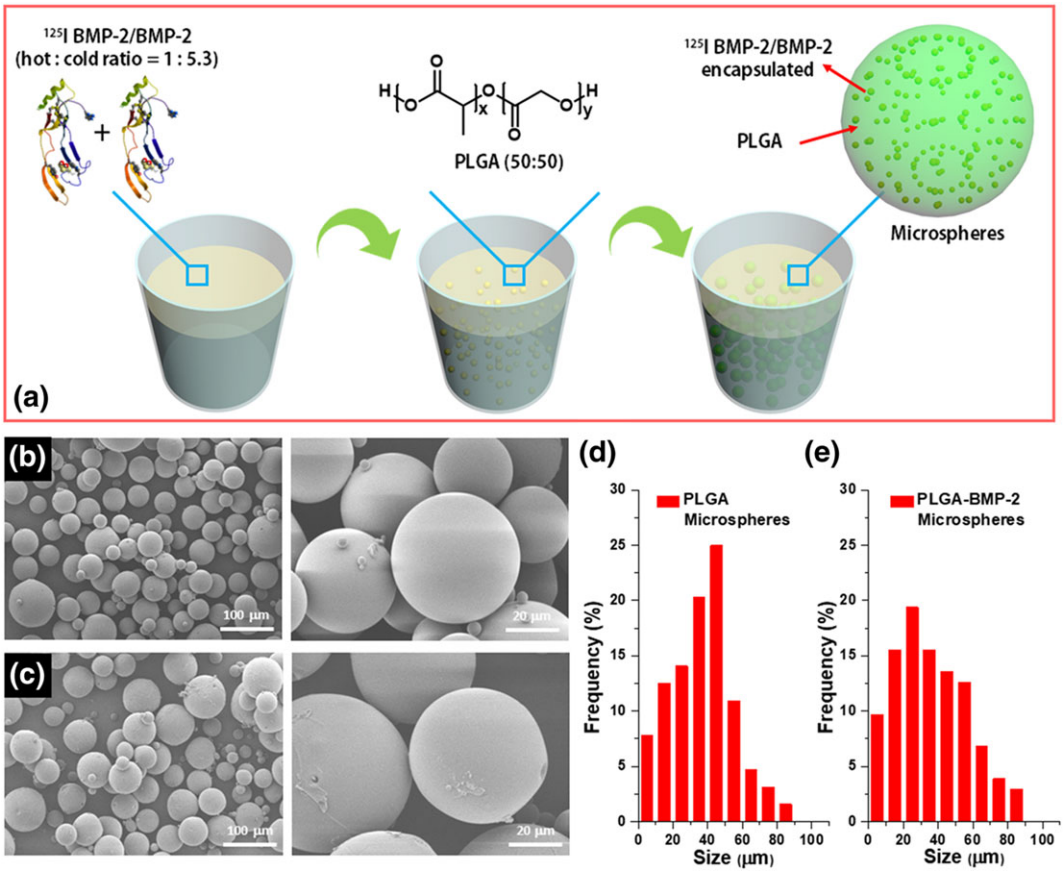

FIGURE 2 (a) Scheme for the fabrication of PLGA microspheres. SEM images of (b) PLGA microspheres and (c) BMP-2-loaded PLGA microspheres. The distribution of (d) PLGA microspheres and (e) BMP-2-loaded microspheres calculated from SEM images. BMP-2, bone morphogenetic protein-2; PLGA, poly(lactic-*co*-glycolic acid); SEM, scanning electron microscopy [Colour figure can be viewed at wileyonlinelibrary.com]

diameter of both the unloaded and loaded microspheres was all distributed between 0 and 100 μm. The detailed distribution profile of the PLGA microspheres was further determined: The PLGA microspheres without BMP-2 showed a sharp distribution profile with the highest peak appearing at around 45 μm (Figure 2d). For PLGA microspheres loaded with BMP-2 protein, however, the distribution was much more even, with the highest peak appearing at around 25 μm and large ratio of particles distributed at 50–70 μm (Figure 2e).

After hydrogel fabrication, the salt in the hydrogel was leached out by soaking in ddH_2O to generate porous hydrogel scaffolds (Figure 3a). A typical hydrogel with salt incorporated is demonstrated in Figure 3b, and the typical porous hydrogel obtained after salt leaching is demonstrated in Figure 3c. The soak volume of OPF-BP was approximately 1.5 times the dry volume of the hydrogel. To determine the salt distribution and porous morphology, the OPF hydrogel, before and after salt leaching, was freeze dried and scoped using SEM. As displayed in Figure 3d, there were obvious salt particles as well as microspheres randomly distributed inside the hydrogel. Leaching out the salt crystals resulted in a randomly distributed microporous structure with PLGA microspheres embedded inside, as presented in Figure 3e.

3.2 | In vitro release kinetics

The release profiles of all composite formulations showed an initial burst release that levelled off to a more sustained release for the rest of the 9 weeks. The BMP-2 loading methods resulted in significantly different burst releases within the first 3 days ($p < .02$). OPF-BP-Msp had released the least BMP-2 within this period (0.4 ± 0.1 μg BMP-2), whereas OPF-BP-Cmb and OPF-BP-Ads had significantly higher

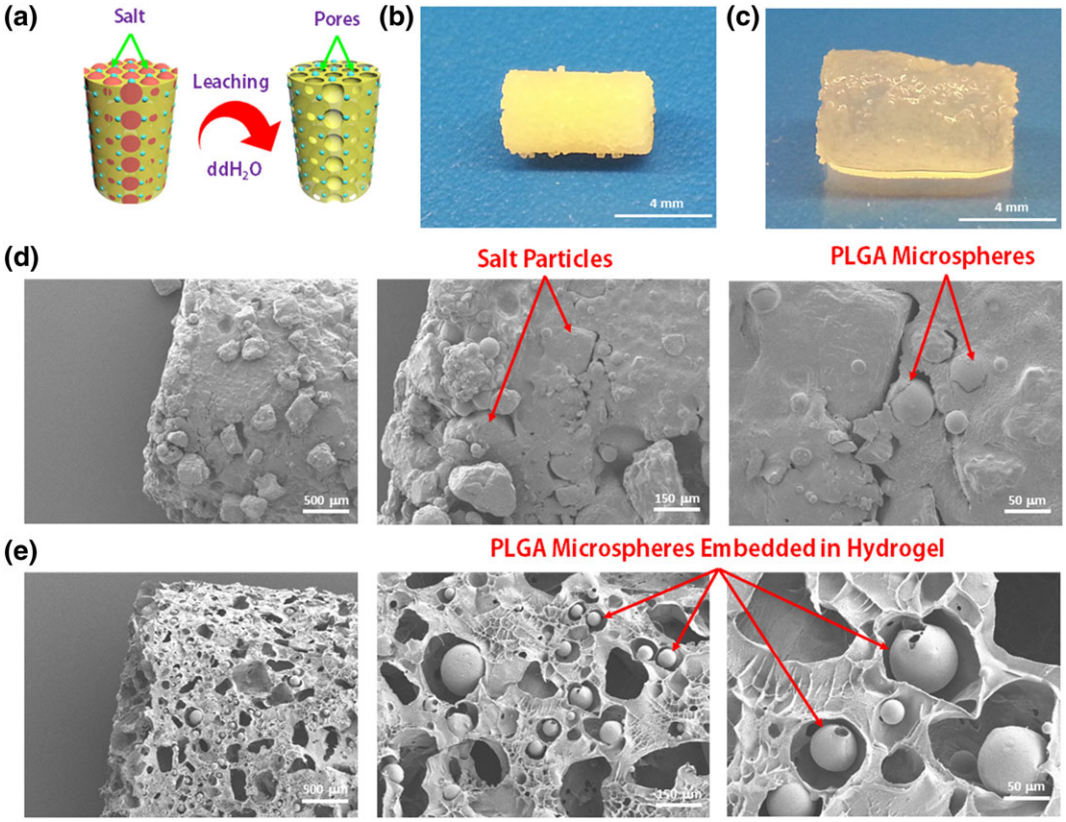

FIGURE 3 (a) Scheme for the salt leaching and pores generation process. Photographs of the OPF-BP composite (b) before and (c) after salt leaching process. SEM images of the OPF-BP composite observed (d) before and (e) after the salt leaching process. ddH_2O, distilled deionized H_2O; OPF-BP, oligo[(polyethylene glycol) fumarate] bis[2-(methacryloyloxy) ethyl] phosphate hydrogel; PLGA, poly(lactic-*co*-glycolic acid); SEM, scanning electron microscopy [Colour figure can be viewed at wileyonlinelibrary.com]

BMP-2 burst releases (0.7 ± 0.2 and 1.1 ± 0.1 µg more, respectively; Figure 4a). A similar release pattern was also observed until Week 3 with OPF-BP-Msp releasing significantly ($p < .02$) less BMP-2 per time-point than did OPF-BP-Cmb and OPF-BP-Ads, while OPF-BP-Ads releasing significantly ($p < .02$) more than did OPF-BP-Cmb. At Week 4, OPF-BP-Ads released significantly ($p < .02$) more BMP-2 than did OPF-BP-Msp and OPF-BP-Cmb. After this time-point, no relevant significant differences were seen between the different OPF-BP formulations.

ACS control group released 1.4 ± 0.09 µg BMP-2 after 3 days (Figure 4a). This was significantly ($p < .008$) higher compared with that of all OPF-BP formulations. BMP-2 release from ACS gradually decreased, resulting in significantly ($p < .006$) less BMP-2 release per time-point compared with that of all OPF-BP formulations from Week 3 till Week 5. After Week 5, no relevant significant differences were seen between ACS and all OPF-BP formulations.

In line with the differential release profile between OPF-BP loading methods, all composites showed significantly ($p < .026$) different cumulative release profiles, with OPF-BP-Msp resulting in a sustained release profile, OPF-BP Cmb in an intermediate release profile, and OPF-BP-Ads and ACS in a predominantly burst release profile, until 4 weeks in culture (Figure 4b). From Week 5 onward, no significant differences ($p > .131$) were found between ACS and OPF-BP-Ads BMP-2 cumulative release. After 9 weeks, 39.8 ± 1.0% BMP-2 was released from OPF-BP-Msp, 55.6 ± 2.5% from OPF-BP-Cmb, 87.2 ± 2.4% from OPF-BP-Ads, and 89.2 ± 2.1% from ACS.

As linear zero-order cumulative release was observed from Week 5 onward, linear regression was used to estimate the BMP-2 release for OPF-BP-Msp and OPF-BP-Ads (+1.1958x + 70.744 with R^2 of 99% and +0.8884x + 20.704 with R^2 of 99%, respectively) after 9 weeks. This showed an expected release of 85.9 ± 37.0 ng for OPF-BP-Msp and 57.3 ± 74.2 ng for OPF-BP-Ads from 9 to 11 weeks.

3.3 | In vitro biological activity in ATDC5 cells

The conditioned medium generated from OPF-BP-Msp and OPF-BP-Ads was still able to generate significantly ($p < 6.3E^{-8}$) higher ALP activity compared with that of the negative control (Figure 4c) after 11 weeks, indicating biological activity of the released BMP-2 in the medium.

ATDC5 cells were responsive to BMP-2 above a concentration of 25 ng/ml of freshly added BMP-2 (positive control). OPF-BP-Msp and OPF-BP-Ads showed significantly ($p < .023$) higher ALP activity (8.3 ± 0.2 and 7.5 ± 1.0 ALP/DNA $U{\cdot}ml^{-1}{\cdot}ng^{-1}$, respectively) than did 25, 50, and 100 ng of freshly added BMP-2 (4.7 ± 0.7, 5.6 ± 0.3 and 6.1 ± 0.8 $U{\cdot}ml^{-1}{\cdot}ng^{-1}$ ALP/DNA, respectively).

3.4 | Animals

Two rats died 1 day after surgery, probably due to oversensitivity to xylazine. No health problems were observed in the reminder of the

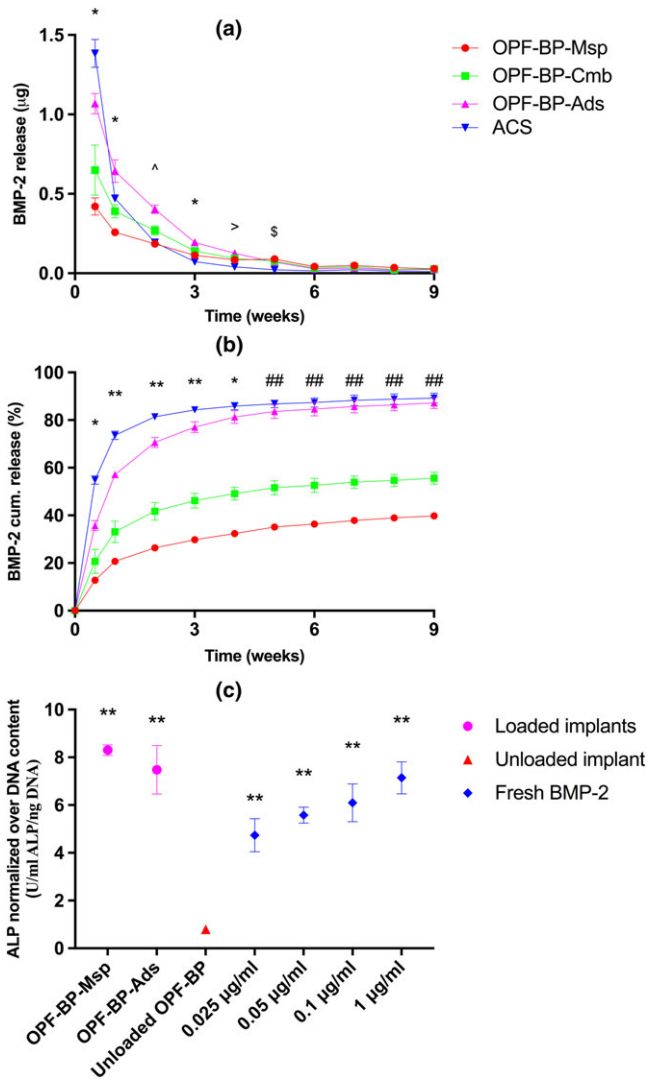

FIGURE 4 In vitro BMP-2 release kinetics (n = 3) from the different composites, shown in (a) µg BMP-2 release and (b) percent BMP-2 cumulative release. (c) ALP activity normalized over total DNA content (U per ml ALP per ng DNA) from ATDC5 cells exposed to conditioned media with OPF-BP implants containing BMP-2 or fresh BMP-2 solution at different concentrations for 3 days. Unloaded OPF-BP implants served as negative control. Significantly different BMP-2 release is indicated between all formulations (*), all formulations except collagen versus OPF-BP-Msp (^), all formulations except OPF-BP-Msp versus OPF-BP-Cmb (>), ACS versus OPF-BP-Msp, OPF-BP-Com and OPF-BP-Ads ($), and all formulations except ACS versus OPF-BP-Ads (#). Significantly different ALP activity versus unloaded OPF-BP control is indicated as *. One symbol indicates a significant difference at $p < 0.05$ and two symbols at $p < 0.01$. OPF-BP, oligo[(polyethylene glycol) fumarate] bis[2-(methacryloyloxy) ethyl] phosphate hydrogel; Msp, microsphere encapsulated BMP-2; Cmb, combined microsphere encapsulated and adsorbed BMP-2; Ads, adsorbed BMP-2; ACS, absorbable collagen sponge; ALP, alkaline phosphatase; BMP-2, bone morphogenetic protein-2 [Colour figure can be viewed at wileyonlinelibrary.com]

rats after the xylazine dose was lowered. Two rats each removed an OPF-BP-Msp implant from their subcutaneous pocket during follow-up, and these implants were discarded from the analysis. No complications were observed in the remainder of the animals.

3.5 | In vivo BMP-2 release

BMP-2 loading methods had a significant effect ($p < .04$) on the BMP-2 burst release from the composites within the first 3 days, with OPF-BP-Msp releasing 1.0 ± 0.4 µg BMP-2, OPF-BP-Cmb releasing 2.0 ± 0.3 µg BMP-2, and OPF-BP-Ads releasing 3.4 ± 0.09 µg BMP-2 (Figure 5a). The amount of BMP-2 loaded in PLGA microspheres correlated inversely with this BMP-2 burst release. ACS showed a burst release of 3.6 ± 0.3 µg BMP-2, which was not significantly different from that of OPF-BP-Ads. During the first week, the release rate of all implants was similar. Subsequently, OPF-BP-Msp and OPF-BP-Cmb released significantly ($p < .01$) more BMP-2 than did OPF-Ads during the second week. OPF-BP-Msp and OPF-BP-Cmb showed again an increase in BMP-2 release per time-point from Week 4 to Week 7. Hereafter, no relevant differences were seen between the implants.

In line with the in vitro results, all OPF-BP composites showed significantly ($p < .007$) different cumulative release profiles, with OPF-BP-Msp resulting in a sustained release profile, OPF-BP Cmb in an intermediate release profile, and OPF-BP-Ads in a burst release profile (Figure 5b). However, whereas OPF-BP-Ads compared with ACS in vitro generated a significantly different release profile, similar cumulative release profiles were seen in vivo. After 9 weeks of implantation, the OPF-BP-Ads and ACS implants released more than 99% BMP-2, whereas OPF-BP-Msp and OPF-BP-Cmb released 88.8 ± 10.4% and 94.6 ± 2.5% BMP-2, respectively.

3.6 | µCT analysis

µCT analysis showed the largest amount of ectopic bone in OPF-BP-Ads (184.4 ± 78.2 mm^3) after 9 weeks of implantation (Figure 5c). The bone volume was significantly ($p \leq .02$) higher than that of OPF-BP-Msp and OPF-BP-Cmb composites. OPF-BP-Msp generated the least volume of bone (0.03 ± 0.01 mm^3), which was significantly ($p = .025$) less than that of OPF-BP-Cmb (67.2 ± 81.2 mm^3) and OPF-BP-Ads. Furthermore, the bone volume in OPF-BP-Ads composites was significantly ($p = .00006$) higher than that of ACS (14.3 ± 8.8 mm^3). Although no significant differences were seen between OPF-BP-Cmb and ACS, the bone volume in the OPF-BP-Msp composites was significantly ($p = .0001$) less than that of ACS.

The 3-D reconstructions confirm this data, with diffuse bone formation seen on the surface and in the pores of the OPF-BP-Cmb and OPF-BP-Ads hydrogels, very minimal bone formation in OPF-Msp, and small compact ossicles for ACS (Figure 5d).

3.7 | Histology

After 9 weeks of implantation, OPF-BP composites containing no BMP-2 (negative control) showed no bone formation with minimal fibrous tissue ingrowth (<50% of the pores filled) and a moderate inflammatory response with some macrophages and multinucleated giant cells (Figure 6a, b, c). OPF-BP-Msp composites showed very minimal osteoid formation and calcifications. Minimal tissue ingrowth mainly consisting of fibrous tissue was seen in less than 50% of the pore volume (Figure 6d, e, f). There was a mild inflammatory response

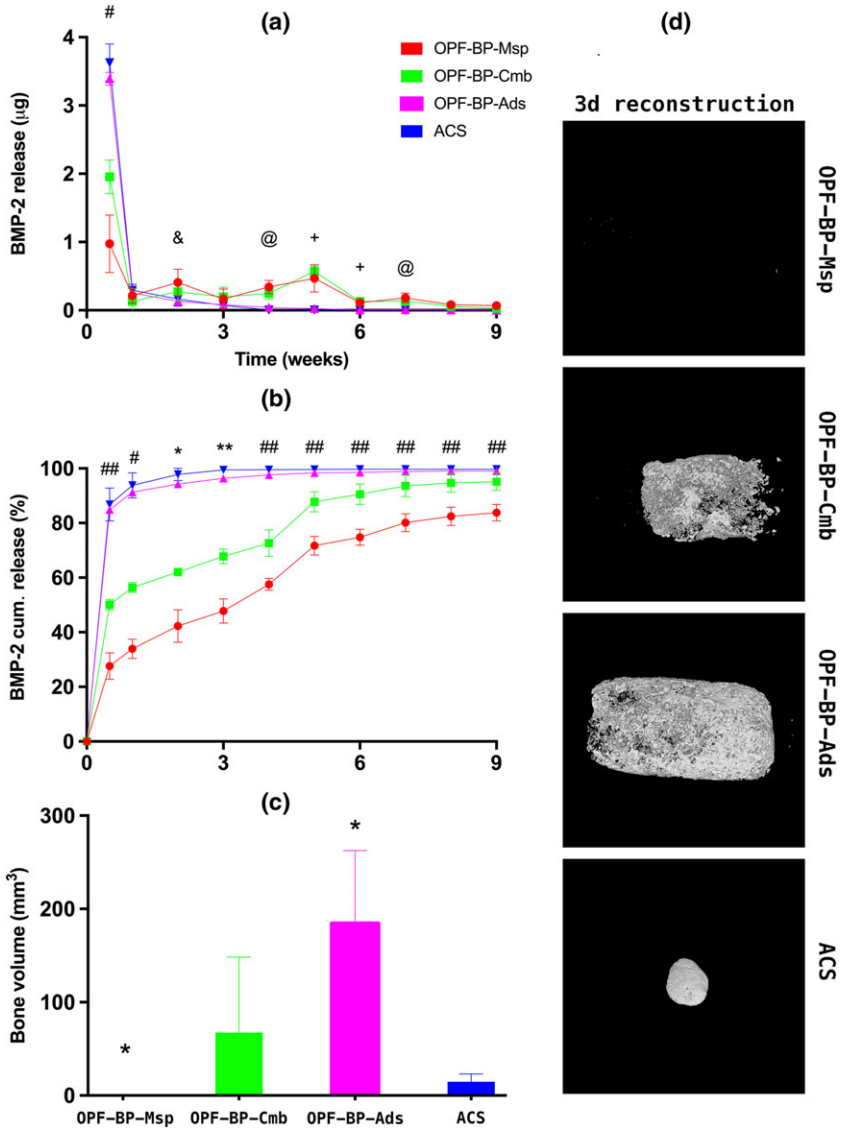

FIGURE 5 In vivo BMP-2 release kinetics (n = 4–8) from the different composites shown in (a) µg BMP-2 release and (b) percent BMP-2 cumulative release. (c) Quantification of the amount of newly formed bone in the four implants, shown in volume mean ± *SD* (mm^3). (d) Three-dimensional µCT reconstructions of the four BMP-2-containing implants after 9 weeks of subcutaneous implantation. Significantly different BMP-2 release is indicated between all formulations (*), all formulations except ACS versus OPF-BP-Ads (#), OPF-BP-Ads versus OPF-BP-Msp and OPF-BP-Cmb (&), OPF-BP-Msp and OPF-BP-Cmb versus OPF-BP-Ads and ACS (@), and ACS versus OPF-BP-Msp and OPF-BP-Cmb, and OPF-BP-Ads versus OPF-BP-Cmb (+). Significantly different bone formation versus all other implants is indicated as *. One symbol indicates a significant difference at $p < 0.05$ and two symbols at $p < 0.01$. OPF-BP, oligo[(polyethylene glycol) fumarate] bis[2-(methacryloyloxy) ethyl] phosphate hydrogel; Msp, microsphere encapsulated BMP-2; Cmb, combined microsphere encapsulated and adsorbed BMP-2; Ads, adsorbed BMP-2; ACS, absorbable collagen sponge; µCT: micro-computed tomography; *SD*, standard deviation; ALP, alkaline phosphatase; BMP-2, bone morphogenetic protein-2 [Colour figure can be viewed at wileyonlinelibrary.com]

in the OPF-BP-Msp composites with few macrophages and multinucleated giant cells. Assessment of OPF-BP-Cmb implanted composites showed good tissue ingrowth (>50% pore volume) with fibrous tissue, osteoid, woven bone, and fat cells. Bone was seen centrally or on the surface of the pores with both fibrous and bone tissue surrounding the exterior of the composite (Figure 6g, h, i). Also these scaffolds showed a mild inflammatory response. OPF-BP-Ads showed good tissue ingrowth (>50%) with mainly osteoid, woven bone, and fat cells. Woven bone was seen on the pores' surface with fat cells centrally showing good integration of the composite and tissue (Figure 6j, k, l). The inflammatory response in the OPF-BP-Ads was minimal compared with that of the previous scaffolds. The ACSs were fully resorbed and replaced by small ossicles with a thin cortex containing trabecular bone structure and fat cells centrally (Figure 6m, n, o).

Fluorescence markers calcein green (green) and tetracycline (orange) showed woven (Figure 7a, c, e, f) and lamellar bone (Figure 7b, d) disposition starting at various locations both early (3 weeks, calcein) and late (6 weeks, tetracycline) in the pores of OPF-BP-Cmb, OPF-BP-Ads, and ACS implants.

4 | DISCUSSION

To investigate the effect of differential BMP-2 release on bone formation, the growth factor was loaded into OPF-BP composites by adsorption and/or microsphere encapsulation. Whereas the chemical and structural properties of the composites were left unchanged, the different BMP-2 loading methods generated significantly different BMP-2 release kinetics. Adsorption mainly resulted in a large burst release with low-dose sustained release of BMP-2 for the rest of the period. Encapsulation of BMP-2 into the microspheres decreased the burst release and resulted in a more sustained release over time. BMP-2 adsorption on the composite matrix resulted in significantly more bone formation than did BMP-2 microsphere encapsulation and the combination of both methods (50% loading in microspheres and 50% loading by adsorption). Although adsorption of BMP-2 into the ACS and OPF-BP composites resulted in similar release profiles, bone formation was 12-fold higher in the OPF-BP-Ads scaffolds than in ACS, a commonly used product in the clinic.

Several mechanisms may be responsible for the incorporation of BMP-2 into the composite including adsorption, ionic complexation,

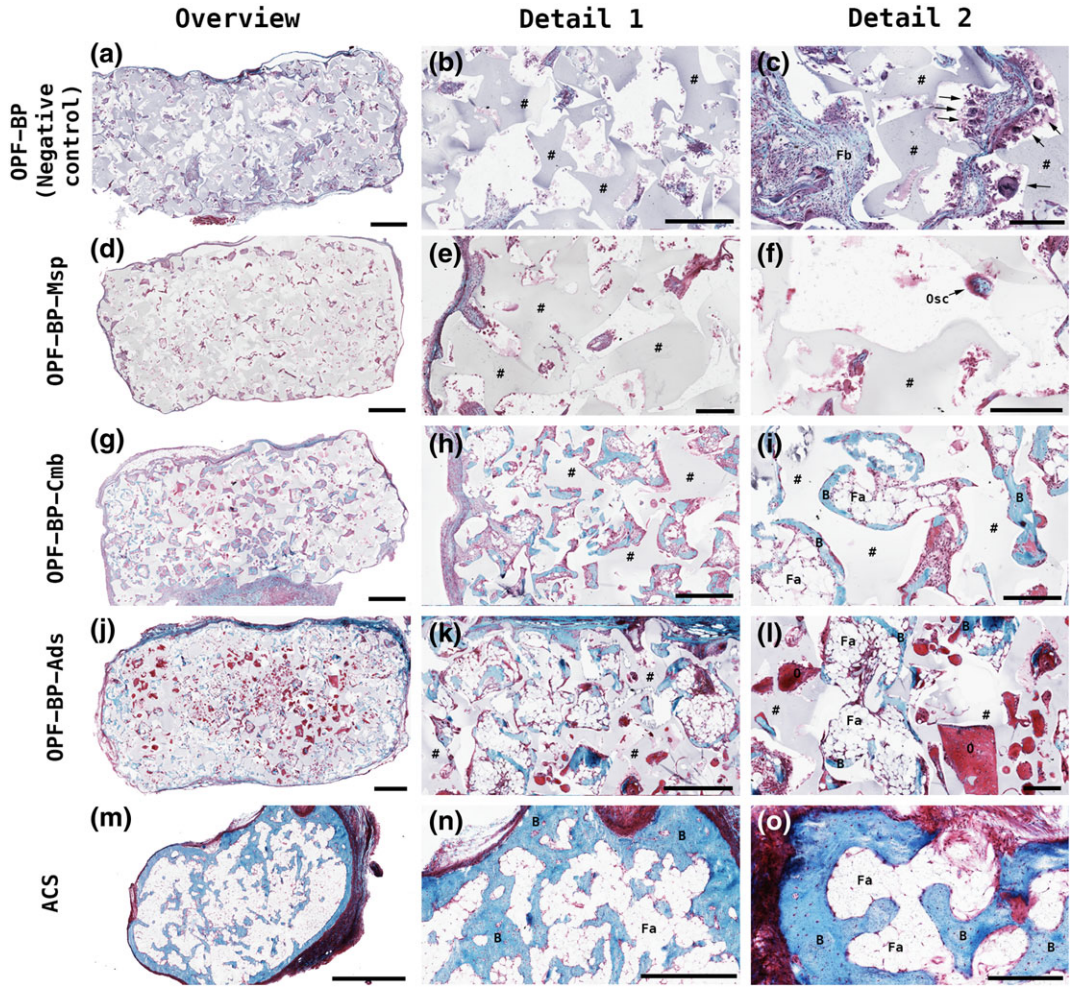

FIGURE 6 Gömöri trichrome stained histological sections of unloaded OPF-BP (negative control; a, b, c), OPF-BP-Msp (d, e, f), OPF-BP-Cmb (g, h, i), OPF-BP-Ads (j, k, l), and ACS (m, n, o) after 9 weeks of subcutaneous implantation. The OPF hydrogel (#) formed an interconnected porous network with minimal fibrous tissue (Fb) ingrowth in unloaded OPF-BP and OPF-BP-Msp. A moderate inflammatory response was in unloaded OPF-BP with some multinucleated giant cells (arrows in c). Whereas only small bony islands (i) were seen in OPF-BP-Msp, good tissue ingrowth was seen in OPF-Cmb and OPF-Ads with bone (b) and osteoid (o) growing on the surface of the hydrogel with fat cells (Fa) centrally in the pores. The ACSs were fully resorbed and replaced by small ossicles with a thin cortex containing trabecular bone structure and fat cells centrally. Scale bars represent 1,000 μm (a, d, g, j, m), 500 μm (B, h, k, n), 200 μm (c, e, i, l, o), and 100 μm (f). OPF-BP, oligo[(polyethylene glycol) fumarate] bis[2-(methacryloyloxy) ethyl] phosphate hydrogel; Msp, microsphere encapsulated BMP-2; Cmb, combined microsphere encapsulated and adsorbed BMP-2; Ads, adsorbed BMP-2; ACS, absorbable collagen sponge [Colour figure can be viewed at wileyonlinelibrary.com]

and physical entrapment. By adsorbing the growth factor onto the composite, the protein binding is dependent on physiochemical interactions and ionic complexation, hence highly sensitive to environmental conditions (Luginbuehl, Meinel, Merkle, & Gander, 2004). In the OPF-BP matrix, rapid desorption and ion exchange in a subcutaneous environment resulted in a BMP-2 burst release of more than 35% in vitro and more than 85% in vivo within 3 days. Microsphere encapsulation and subsequent embedding in the hydrogel matrix resulted in physically entrapped BMP-2 in the composite matrix. This additional diffusion barrier reduced the BMP-2 burst release to approximately 25%, generating a sustained release profile. As the PLGA used in this study lost approximately 80% of its mass within 4 weeks after implantation and BMP-2 release is extended for a longer period, the growth factor entrapment within the OPF-BP hydrogel may also have contributed to BMP-2 retention (Shive & Anderson, 1997).

PLGA microspheres have been used previously to deliver BMP-2 in different biomaterials (Bodde et al., 2008, Hernandez et al., 2012, Woo et al., 2001, Reyes et al., 2014, Reyes et al., 2014, Kempen et al., 2008b). Although PLGA characteristics did not vary much between these studies, the implanted biomaterials showed a wide variation of in vitro and in vivo release profiles. This illustrates that not only the microspheres but also the composite matrix containing them influence BMP-2 release. Although the in vitro release profile can provide valuable information on the growth factor retention mechanisms, the results of this study and previous studies (Hernandez et al., 2012, Kempen et al., 2008b, Piskounova, Gedda, Hulsart-Billstrom, Hilborn, & Bowden, 2014, Rodriguez-Evora et al., 2013, Ruhe et al., 2006, van de Watering et al., 2012, Woo et al., 2001, Yamamoto et al., 2001) show that they greatly underestimate the in vivo release. Comparison of the in vivo release profiles showed that BMP-2 microsphere encapsulation in porous OPF-BP generated a larger burst release than

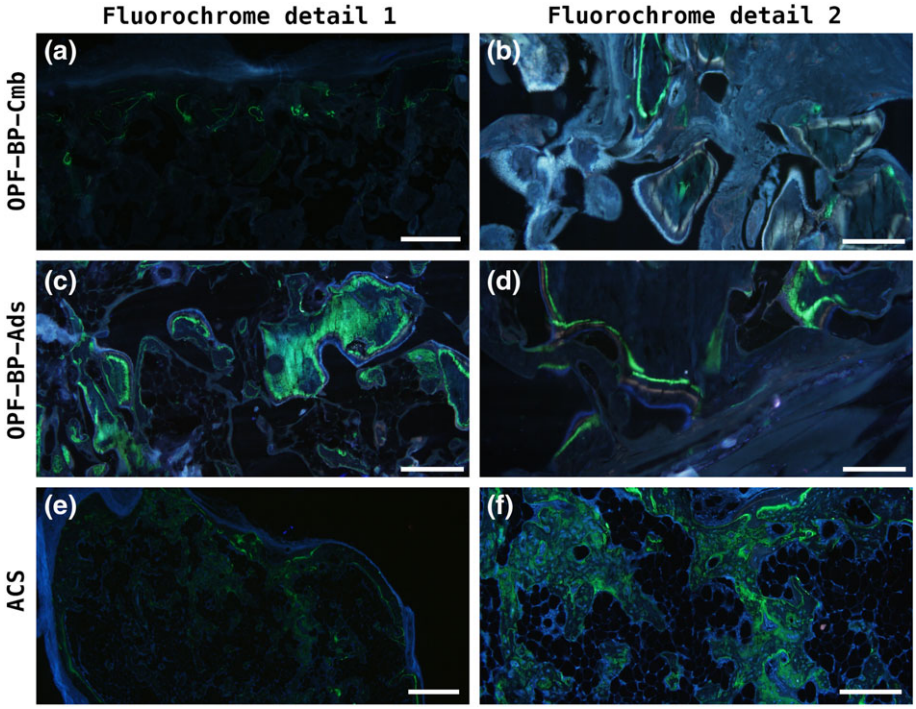

FIGURE 7 Fluorescence imaging of histological samples of OPF-BP-Cmb (a, b), OPF-Ads (c, d), and ACS (e, f). Fluorescence markers calcein green (green) and tetracycline (orange) show woven and lamellar bone disposition in the pores in all BMP-2-containing implants. Scale bars represent 400 μm (a, e), 200 μm (c, f), and 100 μm (b, d). OPF-BP, oligo[(polyethylene glycol) fumarate] bis[2-(methacryloyloxy) ethyl] phosphate hydrogel; Cmb, combined microsphere encapsulated and adsorbed BMP-2; Ads, adsorbed BMP-2; ACS, absorbable collagen sponge [Colour figure can be viewed at wileyonlinelibrary.com]

did solid gelatin, poly(propylene fumarate) (PPF), and calcium phosphate composites containing microspheres (Kempen et al., 2008b, van de Watering et al., 2012). Furthermore, similar subsequent sustained release profiles were seen compared with that of the gelatin–microsphere and PPF–microsphere composites. Kempen et al., 2008b BMP-2 adsorption generated high burst releases (>85%) in both OPF-BP composites and ACS. This was comparable with those of previous studies using ACS implants showing a BMP-2 burst release ranging from approximately 55% to 90% within 3 days and subsequent low-dose sustained releases for another 2–3 weeks (Yamamoto et al., 2003, Uludag, Gao, Porter, Friess, & Wozney, 2001, Uludag et al., 1999, Uludag et al., 2000, Taghavi et al., 2010, Seeherman, Li, Bouxsein, & Wozney, 2010, Friess et al., 1999, Bouxsein et al., 2001, Boerckel et al., 2011).

As prolonged retention in the composite may affect the stability and subsequent biological activity of the growth factor, the in vitro BMP-2 bioactivity was also investigated in this study. The BMP-2 released from both adsorbed and microsphere loading was shown to be biologically active even after 9 weeks. In line with this observation, the bioactivity of BMP-2 released from microspheres, microsphere–gelatin, and microsphere–PPF was already shown over a period of more than 10 weeks (Kempen et al., 2008b). As the biological activity of the protein closely depends on its structural integrity, the results of the present study indicate that a substantial fraction of the protein can remain stable over time within the composite matrix in an in vitro physiologic environment. Given this, it is tempting to hypothesize that this may also be the case in vivo as BMP-2-loaded composites effectively augmented bone formation.

As the chemistry and structure of all OPF-BP composite implants were similar, the differential release profiles could be directly correlated with in vivo bone forming capacity of the released BMP-2. BMP-2 burst release generated significantly more bone than did sustained release in OPF-BP composite implants. Furthermore, the burst release was in direct correlation with bone formation in these implants. The local concentration of BMP-2 achieved by burst release may be one of the key factors for augmented bone formation. Several studies proved that local retention of BMP-2 using carriers improved BMP-2 osteogenic capacity compared with that of injection of carrier-free BMP-2 (Hosseinkhani, Hosseinkhani, Khademhosseini, & Kobayashi, 2007; Rodriguez-Evora et al., 2013; Yamamoto et al., 2003; Yamamoto, Tabata, & Ikada, 1998). Consequently, delivery vehicles are required for a more efficient use of BMP-2. Various BMP-2 release profiles have shown good bone formation in several biomaterials. Low BMP-2 burst release (<5%) with subsequent sustained release showed good bone formation in PPF and calcium phosphate cement (Kempen et al., 2008b, Bodde et al., 2008). Good bone formation was seen in PLGA, brushite, segmented polyurethane/PLGA/beta tricalcium phosphate, gelatin/tricalcium phosphate, insoluble bone matrix, and fibrous glass membrane exhibiting a moderate BMP-2 burst release (20–65%) with subsequent sustained release (Hernandez et al., 2012; Rodriguez-Evora et al., 2013; Takahashi, Yamamoto, & Tabata, 2005; Takita et al., 2004). Finally, also a high BMP-2 burst release (>75%) from collagen and gelatin generated bone (Uludag et al., 2000; Yamamoto et al., 1998). However, few studies attempted to investigate the effect of pharmacokinetic characteristics of BMP-2 release on bone formation in biomaterials with similar chemistry and

structure. Whereas a BMP-2 burst release from calcium phosphate cement implants generated bone, two loading methods resulting in sustained release of BMP-2 did not show any bone formation (van de Watering et al., 2012).

In another study, the cross-linking density of gelatin hydrogels was increased to increase degradation time and hence decreased the BMP-2 burst release (Yamamoto et al., 2003). Initially, BMP-2-induced ALP and osteocalcin in the tissue surrounding the gelatin implants increased with prolonged growth factor retentions. However, above a certain BMP-2 retention, osteoinductivity as well as cell infiltration in the densely cross-linked hydrogel started to decrease. Subsequently, BMP-2 release from two differentially cross-linked gelatin hydrogels was analyzed (Kimura et al., 2009). Whereas both formulations generated a similar small burst release (<20%), the densely cross-linked gelatin showed a more sustained BMP-2 release profile and more de novo bone formation than did the cross-linked gelatin. Furthermore, BMP-2 burst release by adsorption compared with sustained release by microsphere encapsulation generated significantly more bone in gelatin composites (Kempen et al., 2008b). Also when the release and osteoinductive capacity of BMP-2 were studied in insoluble bone matrix and fibrous glass carriers, higher burst release in insoluble bone matrix increased BMP-2 osteoinductivity (Takita et al., 2004). It should be taken into account that the composite modifications could also have influenced the osteoinductive effect of BMP-2 in these studies. Altogether, these studies and the present study suggest that an initial burst release is favourable for ectopic bone formation. However, as studies that are able to directly correlate BMP-2 release and bone formation are very limited, it remains unknown weather this applies to all types of biomaterials.

Apart from the release characteristics, this study also shows that biomaterial characteristics play an important role during bone regeneration. ACS compared with OPF-BP-Ads showed a similar release profile. Therefore, the higher amount of bone formed in the OPF-BP-Ads is most likely due to differences in biomaterial properties. This difference could be due to physical, biomechanical, and chemical properties of the biomaterials. Whereas hydration of OPF-BP results in expansion of its volume of 1.5 times the dry volume, previous characterization of the ACS has shown that the sponge shrinks and loses its geometric conformation with significant smaller pores and approximately one third of soak volume after application of aqueous solution compared with the dry volume (Friess et al., 1999). Previous biomechanical studies showed that the compressive modulus of the phosphorylated OPF-BP lies three times higher than that of the ACS. (Arpornmaeklong, Pripatnanont, & Suwatwirote, 2008; Dadsetan et al., 2012). This allows the OPF-BP to maintain its volume when exposed to external pressure in the subcutaneous in vivo environment. Furthermore, the phosphate in the OPF-BP matrix could have also contributed to the enhanced bone formation. Previous studies have shown that incorporation of phosphate into OPF or poly(ethylene glycol) improved mineralization, and attachment and proliferation of mesenchymal stem cells and osteoblasts in vitro (Dadsetan et al., 2012; Dalby et al., 2007; Muller et al., 2008; Nuttelman, Benoit, Tripodi, & Anseth, 2006). In vivo, an improved osteoconduction and BMP-2-induced bone formation was seen for phosphorylated OPF compared with unmodified (Olthof et al., 2017). Altogether, these findings imply that the role of OPF-BP as an osteoconductive scaffold with its specific physical, biomechanical, and chemical properties could be responsible for the diffuse bone formation in its porous structure as opposed to the small ossicles of mature bone formed from ACS.

5 | CONCLUSION

In conclusion, this study clearly shows that BMP-2 burst release generates more bone than did sustained release in OPF-BP composites. This highlights that the release profile is an important factor influencing BMP-2-induced bone formation. Furthermore, the OPF-BP composite had a similar burst release profile to the clinically used ACS BMP-2 carrier but showed a <12-fold increase in bone formation. This emphasizes that composites should not only function as a delivery vehicle but also provide a proper framework to achieve appropriate bone formation.

ACKNOWLEDGEMENTS

We thank Dr. Nynke Ankringa, ECVP board-eligible veterinary pathologist of the Faculty of Veterinary Medicine at the University of Utrecht, for her assistance during the histological analysis. We also thank James L. Herrick and Carl T. Gustafson of Mayo Clinic for technical support. The authors wish to acknowledge the National Institutes of Health (R01 AR45871 and R01 EB03060), the AO Foundation (AO startup Grant S-15-46K), the Dutch Arthritis Foundation (LLP22), and Anna-NOREF Foundation for their financial support.

CONFLICT OF INTEREST

The authors declare no conflict of interest.

AUTHOR CONTRIBUTIONS

M.G.L.O., L.L., M.J.Y., W.J.A.D., and D.H.R.K designed the study. M.G.L.O., L.L., X.L., M.A.T., and D.H.R.K. participated in data acquisition, analysis, and interpretation. All authors participated in drafting and revising the paper.

ORCID

Maurits G.L. Olthof http://orcid.org/0000-0002-6010-2100

REFERENCES

Aro, H. T., Govender, S., Patel, A. D., Hernigou, P., Perera de Gregorio, A., Popescu, G. I., … Valentin, A. (2011). Recombinant human bone morphogenetic protein-2: A randomized trial in open tibial fractures treated with reamed nail fixation. *The Journal of Bone and Joint Surgery. American Volume*, *93*, 801–808.

Arpornmaeklong, P., Pripatnanont, P., & Suwatwirote, N. (2008). Properties of chitosan–collagen sponges and osteogenic differentiation of rat-bone-marrow stromal cells. *International Journal of Oral and Maxillofacial Surgery*, *37*, 357–366.

Benglis, D., Wang, M. Y., & Levi, A. D. (2008). A comprehensive review of the safety profile of bone morphogenetic protein in spine surgery. *Neurosurgery*, *62*, ONS423–ONS431.

Bodde, E. W., Boerman, O. C., Russel, F. G., Mikos, A. G., Spauwen, P. H., & Jansen, J. A. (2008). The kinetic and biological activity of different loaded rhBMP-2 calcium phosphate cement implants in rats. *Journal of Biomedical Materials Research. Part A*, *87*, 780–791.

Boerckel, J. D., Kolambkar, Y. M., Dupont, K. M., Uhrig, B. A., Phelps, E. A., Stevens, H. Y., … Guldberg, R. E. (2011). Effects of protein dose and delivery system on BMP-mediated bone regeneration. *Biomaterials*, *32*, 5241–5251.

Bouxsein, M. L., Turek, T. J., Blake, C. A., D'augusta, D., Li, X., Stevens, M., … Wozney, J. M. (2001). Recombinant human bone morphogenetic protein-2 accelerates healing in a rabbit ulnar osteotomy model. *The Journal of Bone and Joint Surgery. American Volume*, *83-a*, 1219–1230.

Carragee, E. J., Hurwitz, E. L., & Weiner, B. K. (2011). A critical review of recombinant human bone morphogenetic protein-2 trials in spinal surgery: emerging safety concerns and lessons learned. *The Spine Journal*, *11*, 471–491.

Dadsetan, M., Giuliani, M., Wanivenhaus, F., Brett Runge, M., Charlesworth, J. E., & Yaszemski, M. J. (2012). Incorporation of phosphate group modulates bone cell attachment and differentiation on oligo(polyethylene glycol) fumarate hydrogel. *Acta Biomaterialia*, *8*, 1430–1439.

Dalby, M. J., Gadegaard, N., Tare, R., Andar, A., Riehle, M. O., Herzyk, P., … Oreffo, R. O. (2007). The control of human mesenchymal cell differentiation using nanoscale symmetry and disorder. *Nature Materials*, *6*, 997–1003.

Dickerman, R. D., Reynolds, A. S., Morgan, B. C., Tompkins, J., Cattorini, J., & Bennett, M. (2007). rh-BMP-2 can be used safely in the cervical spine: Dose and containment are the keys! *The Spine Journal*, *7*, 508–509.

Friess, W., Uludag, H., Foskett, S., & Biron, R. (1999). Bone regeneration with recombinant human bone morphogenetic protein-2 (rhBMP-2) using absorbable collagen sponges (ACS): Influence of processing on ACS characteristics and formulation. *Pharmaceutical Development and Technology*, *4*, 387–396.

Friess, W., Uludag, H., Foskett, S., Biron, R., & Sargeant, C. (1999). Characterization of absorbable collagen sponges as rhBMP-2 carriers. *International Journal of Pharmaceutics*, *187*, 91–99.

Garrison, K. R., Donell, S., Ryder, J., Shemilt, I., Mugford, M., Harvey, I., & Song, F. (2007). Clinical effectiveness and cost-effectiveness of bone morphogenetic proteins in the non-healing of fractures and spinal fusion: A systematic review. *Health Technology Assessment*, *11*, 1–150. iii-iv

Gruber, R., Weich, H. A., Dullin, C., & Schliephake, H. (2009). Ectopic bone formation after implantation of a slow release system of polylactic acid and rhBMP-2. *Clinical Oral Implants Research*, *20*, 24–30.

Hernandez, A., Sanchez, E., Soriano, I., Reyes, R., Delgado, A., & Evora, C. (2012). Material-related effects of BMP-2 delivery systems on bone regeneration. *Acta Biomaterialia*, *8*, 781–791.

Hosseinkhani, H., Hosseinkhani, M., Khademhosseini, A., & Kobayashi, H. (2007). Bone regeneration through controlled release of bone morphogenetic protein-2 from 3-D tissue engineered nano-scaffold. *Journal of Controlled Release*, *117*, 380–386.

Kempen, D. H., Lu, L., Classic, K. L., Hefferan, T. E., Creemers, L. B., Maran, A., … Yaszemski, M. J. (2008a). Non-invasive screening method for simultaneous evaluation of in vivo growth factor release profiles from multiple ectopic bone tissue engineering implants. *Journal of Controlled Release*, *130*, 15–21.

Kempen, D. H., Lu, L., Hefferan, T. E., Creemers, L. B., Maran, A., Classic, K. L., … Yaszemski, M. J. (2008b). Retention of in vitro and in vivo BMP-2 bioactivities in sustained delivery vehicles for bone tissue engineering. *Biomaterials*, *29*, 3245–3252.

Kimura, Y., Miyazaki, N., Hayashi, N., Otsuru, S., Tamai, K., Kaneda, Y., & Tabata, Y. (2009). Controlled release of bone morphogenetic protein-2 enhances recruitment of osteogenic progenitor cells for de novo generation of bone tissue. *Tissue Engineering Part A*, *16*, 1263–1270.

Luginbuehl, V., Meinel, L., Merkle, H. P., & Gander, B. (2004). Localized delivery of growth factors for bone repair. *European Journal of Pharmaceutics and Biopharmaceutics*, *58*, 197–208.

Matsumoto, G., Ueda, T., Shimoyama, J., Ijiri, H., Omi, Y., Yube, H., … Mori, H. (2012). Bone regeneration by polyhedral microcrystals from silkworm virus. *Scientific Reports*, *2*, 935.

Muller, P., Bulnheim, U., Diener, A., Luthen, F., Teller, M., Klinkenberg, E. D., … Rychly, J. (2008). Calcium phosphate surfaces promote osteogenic differentiation of mesenchymal stem cells. *Journal of Cellular and Molecular Medicine*, *12*, 281–291.

Nuttelman, C. R., Benoit, D. S., Tripodi, M. C., & Anseth, K. S. (2006). The effect of ethylene glycol methacrylate phosphate in PEG hydrogels on mineralization and viability of encapsulated hMSCs. *Biomaterials*, *27*, 1377–1386.

Olthof, M. G. L., Tryfonidou, M., Liu, X., Pouran, B., Meij, B., Dhert, W., … Kempen, D. H. R. (2017). Phosphate functional groups improve OPF osteoconduction and BMP-2 osteoinductive efficacy. *Tissue Engineering Part A*.

Piskounova, S., Gedda, L., Hulsart-Billstrom, G., Hilborn, J., & Bowden, T. (2014). Characterization of recombinant human bone morphogenetic protein-2 delivery from injectable hyaluronan-based hydrogels by means of ^{125}I-radiolabelling. *Journal of Tissue Engineering and Regenerative Medicine*, *8*, 821–830.

Poduslo, J. F., Curran, G. L., & Berg, C. T. (1994). Macromolecular permeability across the blood–nerve and blood–brain barriers. *Proceedings of the National Academy of Sciences of the United States of America*, *91*, 5705–5709.

Reyes, R., Delgado, A., Sanchez, E., Fernandez, A., Hernandez, A., & Evora, C. (2014). Repair of an osteochondral defect by sustained delivery of BMP-2 or TGFbeta1 from a bilayered alginate-PLGA scaffold. *Journal of Tissue Engineering and Regenerative Medicine*, *8*, 521–533.

Reyes, R., delgado, A., Solis, R., Sanchez, E., Hernandez, A., San Roman, J., & Evora, C. (2014). Cartilage repair by local delivery of transforming growth factor-beta1 or bone morphogenetic protein-2 from a novel, segmented polyurethane/polylactic-*co*-glycolic bilayered scaffold. *Journal of Biomedical Materials Research. Part A*, *102*, 1110–1120.

Rodriguez-Evora, M., Delgado, A., Reyes, R., Hernandez-Daranas, A., Soriano, I., San Roman, J., & Evora, C. (2013). Osteogenic effect of local, long versus short term BMP-2 delivery from a novel SPU-PLGA-betaTCP concentric system in a critical size defect in rats. *European Journal of Pharmaceutical Sciences*, *49*, 873–884.

Ruhe, P. Q., Boerman, O. C., Russel, F. G., Mikos, A. G., Spauwen, P. H., & Jansen, J. A. (2006). In vivo release of rhBMP-2 loaded porous calcium phosphate cement pretreated with albumin. *Journal of Materials Science. Materials in Medicine*, *17*, 919–927.

Seeherman, H., Li, R., & Wozney, J. (2003). A review of preclinical program development for evaluating injectable carriers for osteogenic factors. *The Journal of Bone and Joint Surgery. American Volume*, *85-A*(Suppl 3), 96–108.

Seeherman, H. J., Li, X. J., Bouxsein, M. L., & Wozney, J. M. (2010). rhBMP-2 induces transient bone resorption followed by bone formation in a nonhuman primate core-defect model. *The Journal of Bone and Joint Surgery. American Volume*, *92*, 411–426.

Shive, M. S., & Anderson, J. M. (1997). Biodegradation and biocompatibility of PLA and PLGA microspheres. *Advanced Drug Delivery Reviews*, *28*, 5–24.

Shukunami, C., Ohta, Y., Sakuda, M., & Hiraki, Y. (1998). Sequential progression of the differentiation program by bone morphogenetic protein-2 in chondrogenic cell line ATDC5. *Experimental Cell Research*, *241*, 1–11.

Taghavi, C. E., Lee, K. B., He, W., Keorochana, G., Murray, S. S., Brochmann, E. J., … Wang, J. C. (2010). Bone morphogenetic protein binding peptide mechanism and enhancement of osteogenic protein-1 induced bone healing. *Spine (Phila Pa 1976)*, *35*, 2049–2056.

Takahashi, Y., Yamamoto, M., & Tabata, Y. (2005). Enhanced osteoinduction by controlled release of bone morphogenetic protein-2 from biodegradable sponge composed of gelatin and beta-tricalcium phosphate. *Biomaterials*, *26*, 4856–4865.

Takita, H., Vehof, J. W., Jansen, J. A., Yamamoto, M., Tabata, Y., Tamura, M., & Kuboki, Y. (2004). Carrier dependent cell differentiation of bone morphogenetic protein-2 induced osteogenesis and chondrogenesis during the early implantation stage in rats. *Journal of Biomedical Materials Research. Part A*, *71*, 181–189.

Tazaki, J., Murata, M., Akazawa, T., Yamamoto, M., Ito, K., Arisue, M., … Tabata, Y. (2009). BMP-2 release and dose-response studies in hydroxyapatite and beta-tricalcium phosphate. *Bio-medical Materials and Engineering*, *19*, 141–146.

Tumialan, L. M., Pan, J., Rodts, G. E., & Mummaneni, P. V. (2008). The safety and efficacy of anterior cervical discectomy and fusion with polyetheretherketone spacer and recombinant human bone morphogenetic protein-2: A review of 200 patients. *Journal of Neurosurgery. Spine*, *8*, 529–535.

Uludag, H., D'augusta, D., Golden, J., Li, J., timony, G., Riedel, R., & Wozney, J. M. (2000). Implantation of recombinant human bone morphogenetic proteins with biomaterial carriers: A correlation between protein pharmacokinetics and osteoinduction in the rat ectopic model. *Journal of Biomedical Materials Research*, *50*, 227–238.

Uludag, H., D'augusta, D., Palmer, R., Timony, G., & Wozney, J. (1999). Characterization of rhBMP-2 pharmacokinetics implanted with biomaterial carriers in the rat ectopic model. *Journal of Biomedical Materials Research*, *46*, 193–202.

Uludag, H., Gao, T., Porter, T. J., Friess, W., & Wozney, J. M. (2001). Delivery systems for BMPs: Factors contributing to protein retention at an application site. *The Journal of Bone and Joint Surgery. American Volume*, *83-A*(Suppl 1), S128–S135.

Van de Watering, F. C., Molkenboer-Kuenen, J. D., Boerman, O. C., van den Beucken, J. J., & Jansen, J. A. (2012). Differential loading methods for BMP-2 within injectable calcium phosphate cement. *Journal of Controlled Release*, *164*, 283–290.

Woo, B. H., Fink, B. F., Page, R., Schrier, J. A., Jo, Y. W., Jiang, G., … Deluca, P. P. (2001). Enhancement of bone growth by sustained delivery of recombinant human bone morphogenetic protein-2 in a polymeric matrix. *Pharmaceutical Research*, *18*, 1747–1753.

Yamamoto, M., Ikada, Y., & Tabata, Y. (2001). Controlled release of growth factors based on biodegradation of gelatin hydrogel. *Journal of Biomaterials Science. Polymer Edition*, *12*, 77–88.

Yamamoto, M., Tabata, Y., & Ikada, Y. (1998). Ectopic bone formation induced by biodegradable hydrogels incorporating bone morphogenetic protein. *Journal of Biomaterials Science. Polymer Edition*, *9*, 439–458.

Yamamoto, M., Takahashi, Y., & Tabata, Y. (2003). Controlled release by biodegradable hydrogels enhances the ectopic bone formation of bone morphogenetic protein. *Biomaterials*, *24*, 4375–4383.

Yao, Y., & Wang, Y. (2013). ATDC5: an excellent in vitro model cell line for skeletal development. *Journal of Cellular Biochemistry*, *114*, 1223–1229.

How to cite this article: Olthof MGL, Kempen DHR, Liu X, et al. Bone morphogenetic protein-2 release profile modulates bone formation in phosphorylated hydrogel. *J Tissue Eng Regen Med*. 2018;12:1339–1351. https://doi.org/10.1002/term.2664